Journal of Materials Processing Technology 212 (2012) 786– 793

Control of wall thickness distribution by oblique shear spinning methods

A. Sekiguchi [a,*,1], H. Arai [b]

[a] Graduate School of Systems and Information Engineering, University of Tsukuba, 1-1-1 Tennohdai, Tsukuba 305-8571, Japan.

[b] Advanced Manufacturing Research Institute, National Institute of Advanced Industrial Science and Technology, 1-2-1 Namiki, Tsukuba 305-8564, Japan.

[*] Corresponding author. Fax.: +81 3 3909 2590. *E-mail address:* sekiguchi.akio@iri-tokyo.jp (A. Sekiguchi).

[1] Present address: Commercialization Support Department, Tokyo Metropolitan Industrial Technology Research Institute, Aomi 2-4-10, Koutou-ku 135-0064, Japan.

ABSTRACT

A flexible method of forming circumferentially variant wall thickness distributions on the same shape is attempted using two oblique sheet spinning processes. The fundamental strategy entails the inclination of the flange plane of the workpiece during forming. In one type of synchronous dieless spinning, edge-hemmed aluminum blanks of 186 mm diameter and 1.5 mm thickness are formed for truncated cone shells of 30 degrees half-angle, by synchronizing the motion of the spherical head roller in the axial and radial directions with the angle of the general purpose mandrel fixed on a bidirectionally rotating spindle. On the other hand, in the other type of force-controlled shear spinning, flat aluminum discs of 150 mm diameter and 1.0 mm thickness are formed by feeding perpendicularly to the flange plane of the workpiece and maintaining the thrust force along the plane via the roller tool, exerted onto the rotating truncated-cone-shaped die of the same half-angle of 30 degrees. The estimated wall-thickness distribution based on a simple shear deformation model nearly conformed to the measured thickness distributions of the products formed at several inclination angles of up to 15 degrees in the forming and both spinning methods.

Keywords: Shear spinning; Sine law; Incremental sheet forming; Thickness distribution control; Deformation behavior.

1. Introduction

Metal spinning is an age-old forming technique for making axisymmetric shell products from metal sheets or tubes. In recent years, the flexibility of spinning has been enhanced as a result of research and development (Music et al. 2010).

A dieless shear spinning method for a sheet metal was developed by Shima et al. (1997), and truncated cone shells were formed by substituting an inner roller for a mandrel. In another approach investigated by Kawai et al. (2001), cone shapes were formed without using a dedicated die by using workpieces with flange of sufficiently high stiffness to suppress shrink flanging at the forming point.

Some asymmetric spinning methods based on the positional control of a spindle and roller(s) have been proposed. Elliptical shaping in shear spinning was archived by Amano and Tamura (1984) by configuring a mechanical synchronous system between a rotating spindle and a roller moving in the radial direction with cams and links. Elliptical spinning was also investigated by Gao et al. (1999) who considered another mechanical setup in which the spindle axis coincident with the revolution is offset. A more flexible spinning machine using a mandrel and a three-dimensional cam was proposed by Qinxiang et al. (2010). The non-axisymmetric spinning of tube blanks was investigated by Arai et al. (2005), who developed a synchronous spinning lathe using a numerical controller that included spindle angle control. Asymmetric shear spinning methods for metal sheets using computerized spinning machines were investigated by Amano et al. (1990), Härtel and Awiszus (2010), and Shimizu (2010).

On the other hand, several asymmetric spinning methods based on force control via roller(s) onto a

mandrel have been proposed. A spinning method for forming convex and concave tripod shapes using a spinning lathe with spring-driven rollers was investigated by Awiszus and Meyer (2005). A shear spinning method using force control was proposed by Arai (2004), and asymmetric products have been formed by force-controlled spinning (Arai 2005).

An oblique spinning method involving a tube blank was proposed by Shindo et al. (1999), who developed a novel spinning lathe in which roller tools are moved while rotating around a tube blank. The forming force in a similar process was investigated Xia et al. (2006) by finite element simulations and trial forming. In incremental sheet forming (Matsubara 1994), forming of curved products which differ from the intended shapes can be achieved through a method developed by Mastubara (1995).

In this study, a flexible method of forming products with variable wall thickness distributions on the same shape using the same blanks is investigated. Inclining the flange plane of the workpiece during the process is the fundamental strategy used in this method.

The conventional spinning of metal sheets and the flow forming of metal tubes are spinning processes in which the axial distribution of the wall thickness of a product is adjustable (Wong et al. 2003). However, it is difficult to adjust the circumferential distribution in metal spinning without using a blank of nonuniform thickness or milling after forming. A spinning method, in which the circumferential distribution can be varied by simply changing the software and in which normal low-cost blanks can be used, may be useful for optimizing the strength per unit weight of the product considering external force distribution, equalizing the thickness distribution in asymmetric forming, and keeping enough the thickness when thread cutting on the wall of the product.

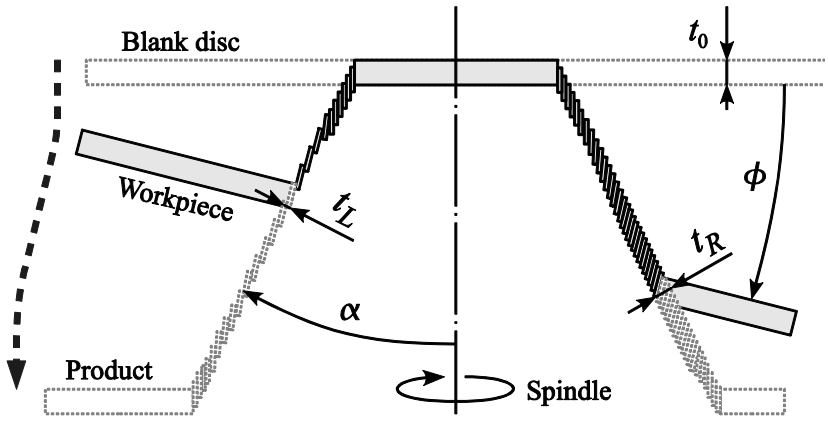

Fig. 1. Relationship among the half-angle α, the inclination angle ϕ, and the wall thicknesses in the oblique shear deformation model.

2. Methodology

In shear spinning, the wall thickness t of a conical product is determined by the half-angle α and the original thickness t_0 of the blank in accordance with the sine law:

$$t = t_0 \sin\alpha. \tag{1}$$

This relation is also valid in previously proposed dieless shear spinning methods (Shima et al. 1997),(Kawai et al. 2001), in which the flange plane of the workpiece is kept flat.

In the case of the dieless shear spinning of curved truncated cone shells, a predictive expression based on shear deformation perpendicular to a progressively inclined flange plane was proposed, and it was verified that the model closely coincides with measured thickness distributions along the outer and inner sides of curved cones (Sekiguchi and Arai 2010a). By applying the model, it is predicted that the wall thickness distribution can be varied while retaining the same shape by altering the inclination angle of its flange plane during the process, as shown in **Fig. 1**. The wall thicknesses on the left and right sides of the product shown in **Fig. 1** are geometrically calculated from the model using the inclination angle ϕ of the flange plane and the following simple equations:

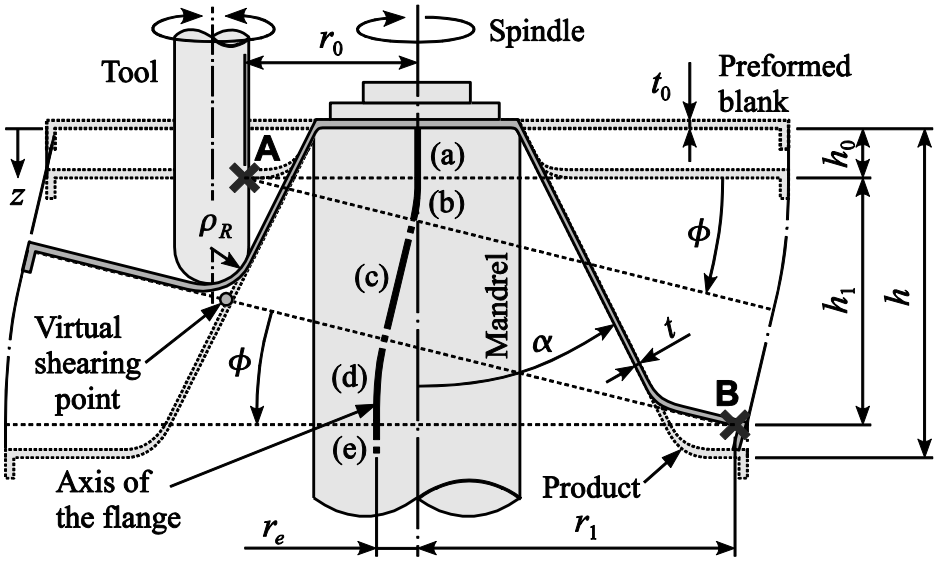

Fig. 2. Schematic of the experiment on controlling the wall thickness distribution in synchronous dieless spinning.

$$\begin{cases} t_L = t_0 \sin(\alpha - \phi) \\ t_R = t_0 \sin(\alpha - \phi) \end{cases}. \tag{2}$$

Similarly to the sine law in Equation (1), according to this equation, a processed wall cannot be thicker than its original thickness, since the ratio of the wall thickness to the original thickness, t/t_0, is $\sin(\alpha \pm \phi) \leq 1$.

In this paper, as indicated in **Fig. 2**, a product is formed in order (a) to (e) by inclining the flange plane at points A and B in the dieless spinning method. Since the workpiece is rotated by a spindle axis, the position of the spherical head roller tool should be controlled synchronously in the radial and axial directions as illustrated in **Fig. 3**. The truncated cone was selected as the simplest product shape to investigate the variation of the wall thickness distribution in this study.

However, since the tip of the roller tool is spherical, the wall thickness estimated using Equation (2) changes with the position of virtual shear deformation. In our preliminary experiments, the wall thickness was estimated along the line intersecting the flange plane and the surface of the intended shape to ensure consistency.

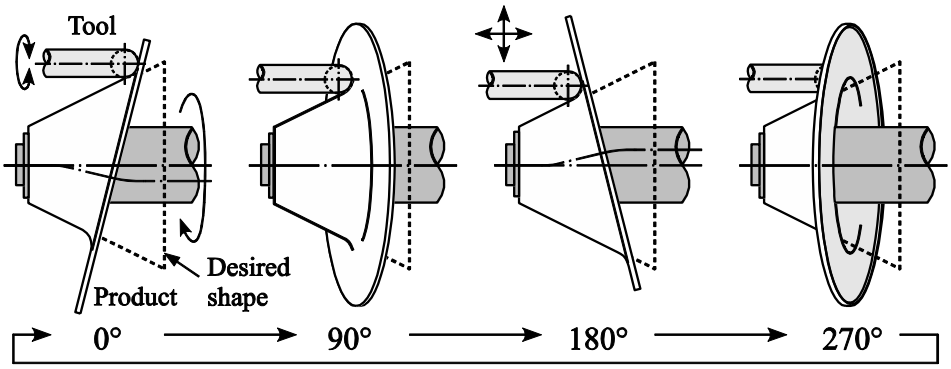

Fig. 3. Synchronous motion of the tool during one rotation of the spindle.

Note that, the oblique forming of a flange plane can also be performed by the force-controlled oblique shear spinning method (Sekiguchi and Arai 2010b), although there are several differences, such as the machine structure, the necessity of a dedicated die, and the control method of the tool. In this study, the deformation behavior of the proposed method was investigated by considering the wall thickness distributions of truncated conical products formed at several inclination angles in comparison with those obtained by the force-controlled oblique shear spinning method.

3. Control of wall thickness distribution in synchronous dieless spinning process

3.1. Experimental Setup

Synchronous dieless spinning was conducted by fixing a roller tool on an XY table and a blank sheet on the spindle axis of a numerically controlled five-axis metal spinning machine. As the tool, a quenched roller with a spherical head of radius ρ_R = 8 mm made of alloy tool steel AISI-SAE D2 was supported parallel to the spindle axis, with bearings installed to allow free rotation. A mandrel of diameter 50 mm and shoulder radius 1 mm was used. Commercially available pure aluminum discs (AA1100-H24) of nominal thickness t_0 = 1.5 mm and outer diameter 200 mm were used as blank sheets. The mechanical properties of the aluminum discs were obtained through tensile tests as shown in **Table 1**. The center of a blank disc was screwed tightly to the tip of the mandrel using a jig,

Table 1

Mechanical properties of aluminum disc of 1.5 mm thickness using specimen #6 of JIS. 2201.

Rolling direction /deg	0	45	90
Elastic modulus /GPa	3.21	2.75	2.85
Proof strength /MPa	96.2	97.8	106
Tensile strength /MPa	122	111	119
Break elongation /%	21.8	24.5	24.1

the rolling direction of which was set to the direction of inclination. The 7-mm-wide edge of the disc was hemmed to 90° in advance by simple conventional spinning so that the flange plane of the workpiece remained flat during forming. Before forming, general purpose lubricant oil was sprayed on the blank.

3.2. Forming Method and Conditions

To move the tool on a suitable roller trajectory in this experiment, as shown in **Fig. 2**, a computer program used in one of our previous studies (Sekiguchi and Arai 2010a) was modified. The tool trajectory was geometrically calculated from the virtual curved axis and the desired profile of the product by obtaining the helical trajectory of the contact point between the spherical-headed tool and the desired profile as it rotates around the virtual curved axis. The required forming time can be estimated simultaneously.

The half-angle α of the truncated cone was set at 30°, to ensure a sufficient forming length for evaluation and to avoid the occurrence of wall fracture that may occur at a smaller half-angle. The height of the product was set at h = 80 mm, the initial forming height was set at h_0 = 15 mm, and the oblique forming height was set at h_1 = 55 mm. The tilting axes of the flange (points A and B in **Fig. 2**) were placed outside the desired profile by setting r_0 = 50 mm and r_1 = 80 mm. In addition, the feed rate of the flange plane along the virtual curved axis was set at p = 0.3 mm·rev^{-1} and the

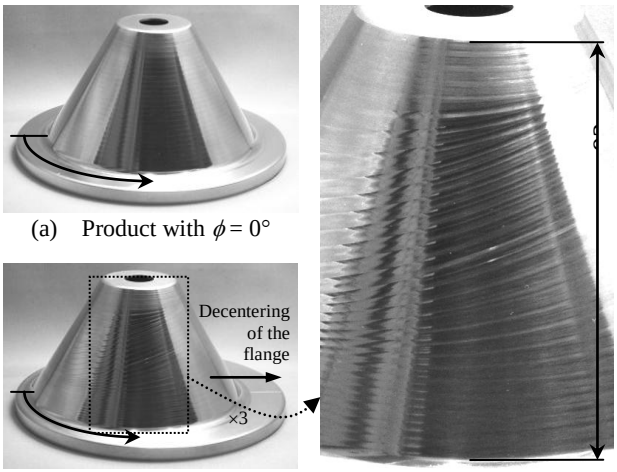

(a) Product with $\phi = 0°$

(b) Product with $\phi = 15°$

(c) Feed marks on the wall

Fig. 4. Comparison of truncated cones with different inclination angles ϕ of the flange in dieless forming.

relative speed at the contact point was set at F = 10,000 mm·min^{-1} to ensure stable forming conditions.

In contrast to normal shear spinning, in the present process it is unavoidable that the density of the feed marks on the wall becomes circumferentially nonconstant as indicated by (b) and (d) in **Fig. 2**. However, the effect of the density variation to the wall thickness can basically be ignored, according to earlier studies, since a change in the axial feed rate does not affect the wall thickness in the dieless shear spinning process (Kawai et al. 2001). In contrast, in the dieless process, the preformed part of the cone is twisted by the circumferential forming force during the process, since the wall is not supported by a die. By reversing the rotational direction of the spindle axis every 6.5 revolutions during forming, the torsion was effectively suppressed for all products in this experiment.

3.3. Appearance and Profile

Truncated cone products with inclination angles of the flange in the oblique forming process of ϕ = 0° and 15° are shown in **Fig. 4**. The forming time was 13.5 min for ϕ = 15°. The outer profiles were burnished owing to rolling/sliding contact with the roller and covered with feed marks owing to the

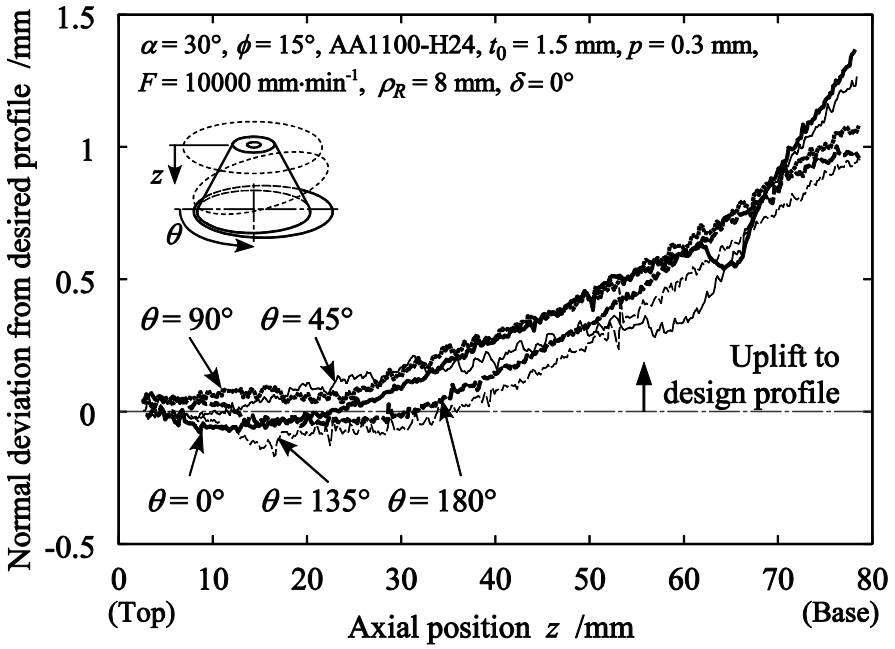

Fig. 5. Normal deviation of the outer profile of the product with ϕ = 15° from the desired profile over half the circumference.

motion error generated by switching the rotational direction of the spindle. The flange planes of the products were radially displaced to left in **Fig. 1** from the original position of the blank. The larger the inclination angle ϕ, the greater the displacement. However, the thickness of the flange was same as its original thickness for all products because the flange was not deformed by the roller. Hence, the displacement indicates that the wall thickness of the products varied circumferentially.

Given that the cone half-angle α is included in Equation (2), it is necessary that the profiles of all products are the same to impartially evaluate the wall thicknesses of the products. **Fig. 5** shows axial distributions of the normal deviation from the desired profile and the measured profile using a laser range sensor, over half the circumference of the product with ϕ = 15°.

At the base of the product, the normal deviation reaches 1 mm because of springback since the roller trajectory is geometrically calculated from the desired profile without taking springback into account. However, the circumferential variation between the profiles is suppressed to about 0.3 mm or less;

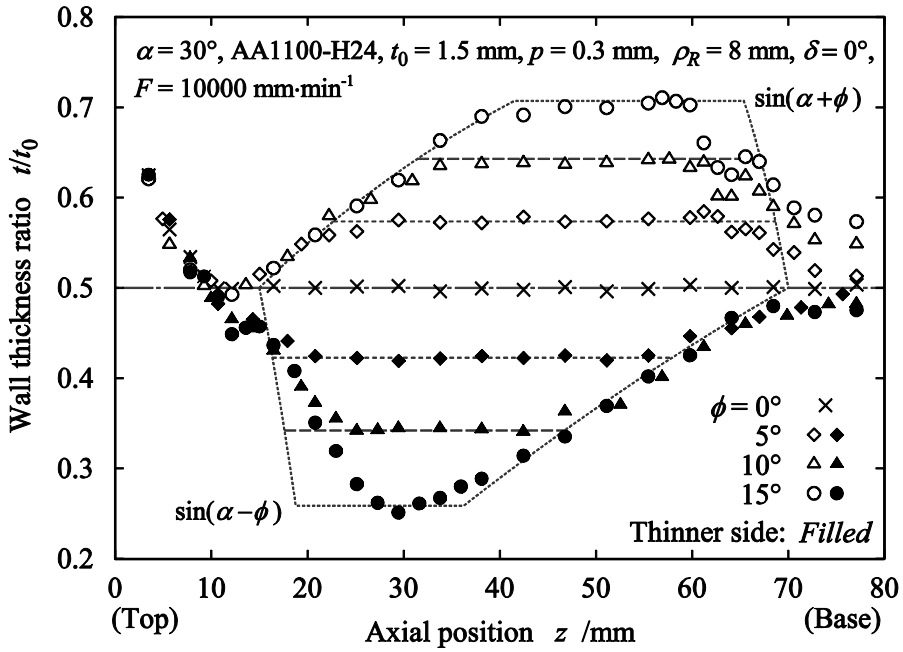

Fig. 6. Axial distributions of wall thickness ratio on thicker and thinner sides for inclination angles ϕ of up to 15°.

this tendency was the same at every inclination angle in this experiment including $\phi = 0°$.

3.4. Axial Distribution of Wall Thickness

Fig. 6 shows axial distributions of the ratio of wall thickness t to original thickness t_0 for inclination angles of $\phi = 0°$, 5°, 10°, and 15°. The ratios for the thinner and thicker sides in **Fig. 1**, t_L/t_0 and t_R/t_0, are indicated by filled marks and open marks, respectively. The thicknesses were measured using a spherical face micrometer. At $\phi = 0°$, t/t_0 was nearly 0.5 in agreement with the sine law (dash-dotted line). For greater inclination angles, the amount of thinning on each side increases or decreases compared with the ratio of the sine law, $t/t_0 = \sin\alpha$. The thickness changes drastically at axial positions of z = 15 mm on the thinner side and z = 65 mm on the thicker side, since the feed marks of the roller become fine near the points A and B in **Fig. 2**.

The dotted lines in **Fig. 6** are predictive distributions calculated from the trajectory of the flange plane (the heavy dash-dotted line in **Fig. 2**) using Equation (2). Although, they did not closely match

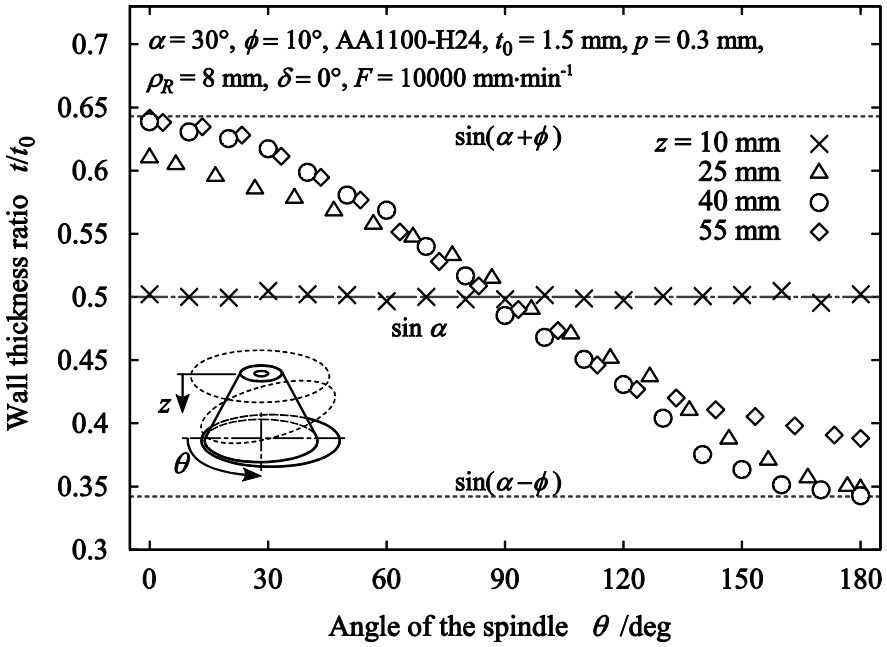

Fig. 7. Circumferential distributions of wall thickness ratio along half circumferences of the cone at various axial positions when $\phi = 10°$.

the thicknesses of the actual products, they are nearly the same on both sides. Hence, the ϕ can be simply configured using the desired thickness ratio t_d/t_0 by the following equation:

$$\phi = \alpha - \sin^{-1}\left(\frac{t_d}{t_0}\right). \tag{3}$$

3.5. Circumferential Distribution of Wall Thickness

Fig. 7 shows circumferential distributions of the thickness ratio t/t_0 along half circumferences of the product with $\phi = 10°$ at distances of z = 10, 25, 40, 55 mm from the top of the product. At z = 40 mm, the distribution is similar to a sinusoidal function whose maximum and minimum values are expressed as $\sin(\alpha \pm \phi)$, whereas at z = 25 mm and z = 55 mm, there is a section where the deviation of the thickness ratio from that predicted by the sine law is less than that when z = 40 mm, since ϕ is smaller at (b) and (d) in **Fig. 2**. Thus, the proposed method does not have the flexibility to control the circumferential distribution. However, the maximum and minimum values of thickness ratio can be

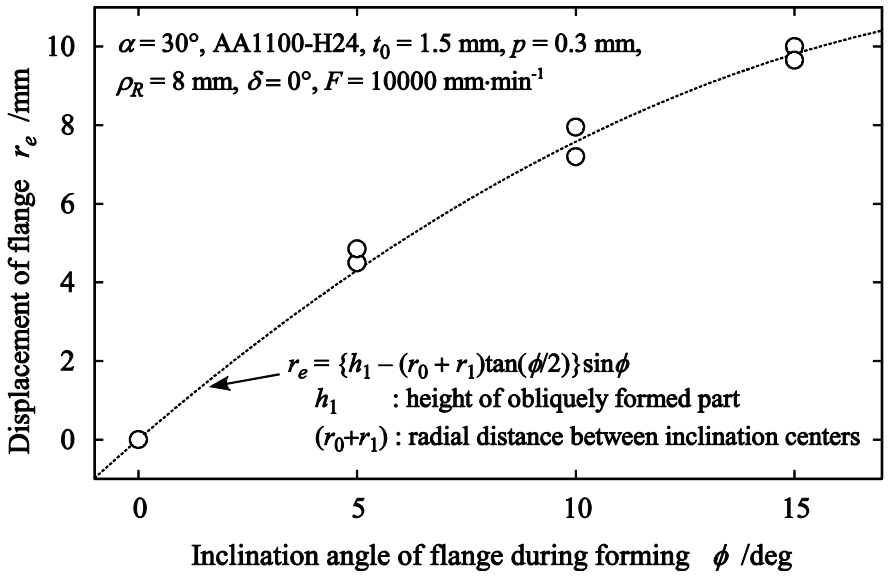

Fig. 8. Relationship between inclination angle ϕ and radial displacement of flange r_e.

estimated.

3.6. Radial Displacement of Flange

It is considered that the radial displacement of the flange give the integrals of the differences between the sine-law thickness and the wall thickness along the thinner side upon multiplying by the original thickness. Thus, if the magnitude of the displacement is known in advance, material wastage can be suppressed by offsetting the radial position of the blank. **Fig. 8** shows the relationship between the inclination angle ϕ and the measured displacement of the flange, r_e. The dotted line is the estimated value geometrically calculated from the trajectory of the flange plane in **Fig. 2**. The measured r_e are closely approximated by the equation

$$r_e = \left\{ h_1 - (r_0 + r_1) \tan \frac{\phi}{2} \right\} \sin \phi . \tag{4}$$

Table 2

Mechanical properties of aluminum disc of 1.0 mm thickness using specimen #6 of JIS. 2201.

Rolling direction /deg	0	45	90
Elastic modulus /GPa	3.44	3.54	3.40
Proof strength /MPa	85.2	83.3	88.9
Tensile strength /MPa	121	109	117
Break elongation /%	23.0	22.8	26.5

4. Control of wall thickness distribution in force-controlled shear spinning process

4.1. Experimental Setup

Force-controlled shear spinning was conducted using a spinning machine consisting of a main spindle for rotating a workpiece with a mandrel and an XY table for moving a roller. A disc-shaped roller made of alloy tool steel AISI-SAE D2 with a nose radius of ρ_R = 8 mm and a diameter of 70 mm was mounted on the XY table at an angle of δ = 30° from the spindle axis and a six-axis force/torque sensor was fixed at the base of the roller. A truncated-cone-shaped mandrel made of stainless steel with a half-angle of α = 30°, a top diameter of 40 mm, and a shoulder radius of 1 mm was used. As a blank, a commercially available pure aluminum disc (AA1100-H24) of nominal thickness t_0 = 1.0 mm and outer diameter 150 mm was selected after considering the rated force (800 N) of the actuators of the XY table. The center of a blank disc was screwed tightly to the tip of the mandrel using a jig, the rolling direction of which was set to the direction of inclination. **Table 2** gives the mechanical properties of the aluminum discs. Before forming, general purpose lubricant oil was sprayed on the blank.

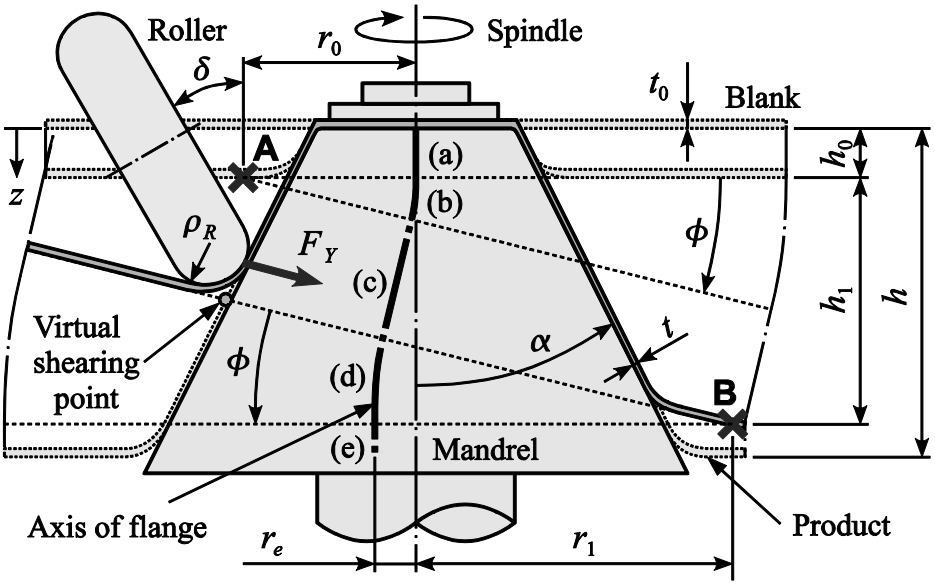

Fig. 9. Schematic of the experiment on controlling the wall thickness distribution in force-controlled shear spinning.

4.2. Forming Method and Conditions

A computer program used in one of our earlier studies (Sekiguchi and Arai 2010b) was modified to conduct the experiment with a suitable tool trajectory as shown in **Fig. 9**. In this spinning method, a product is formed in order (a) to (e) in **Fig. 9** while maintaining the centripetal force parallel to the flange plane, F_Y, at a constant value using a force-control method and constraining the tip of the roller on the plane, as illustrated in **Fig. 10**. Owing to the rotation of the workpiece on the spindle, the coordinate system used in the force/position control of the roller is tilted depending on the inclination angle ϕ of the plane and the rotational angle θ of the spindle. Unlike the former dieless spinning method, designing a three-dimensional trajectory for the roller using CAM-like software in advance is not necessary in the present method, since the desired trajectory is dynamically calculated during the process in accordance with the profile of the mandrel.

The half-angle α of the products was set at 30° by the mandrel, the same as in the previous experiment. The height of the products, h = 60 mm, the initial forming height h_0 = 10 mm, and the

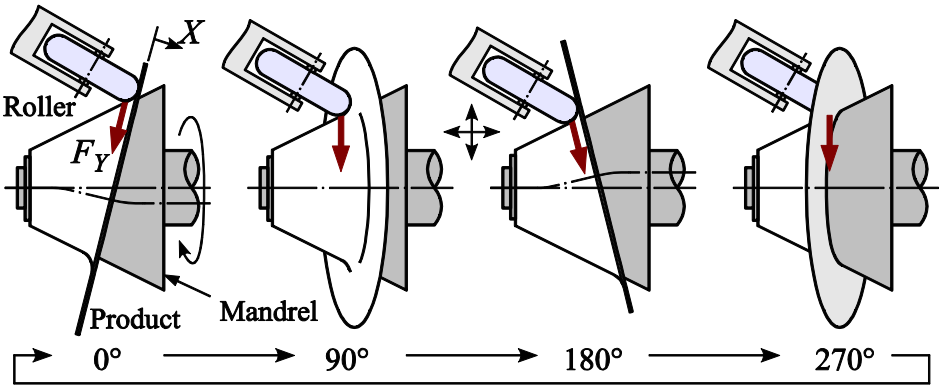

Fig. 10. Motion of the roller and the constant-force direction during one rotation in force-controlled shear spinning.

oblique forming height h_1 = 50 mm were selected after consideration of the sizes of the mandrel and blank. The tilting axis of the flange, points A and B in **Fig. 9**, were placed opposite each other at radial distances of r_0 = 40 mm and r_1 = 70 mm. The feed of the roller per revolution when the inclination angle is constant was set at p = 0.4 mm·rev^{-1} and the feed when the angle is changing at (b) and (d) in **Fig. 9** was set at p_A = 0.5 °·rev^{-1} and p_B = 0.4 °·rev^{-1}. The spindle speed was set at ω = 30 rpm. The initial 4 mm of h_0 was formed using positional control. The rotational direction of the spindle was not switched, in contrast to the previous experiment on synchronous dieless spinning. The desired centripetal force of the roller was determined as F_Y = 550 N with reference to an earlier study by Arai (2005).

4.3. Appearance, Profile, and Forces

Truncated cone products, with inclination angles of the flange in the spinning process of ϕ = 0° and 15° are shown in **Fig. 11**. The forming time was 5 min 10 s for ϕ = 15°. The outer surfaces of the products were covered with glossy feed marks following the roller trajectory, while the inner surfaces were smooth owing to the pressure of the mandrel. Slight depressions were observed near the points A and B in **Fig. 9**, since the roller tracks on the inner surface of the inclination of the flange were considerably finer than those on the outer surface. The flange planes were

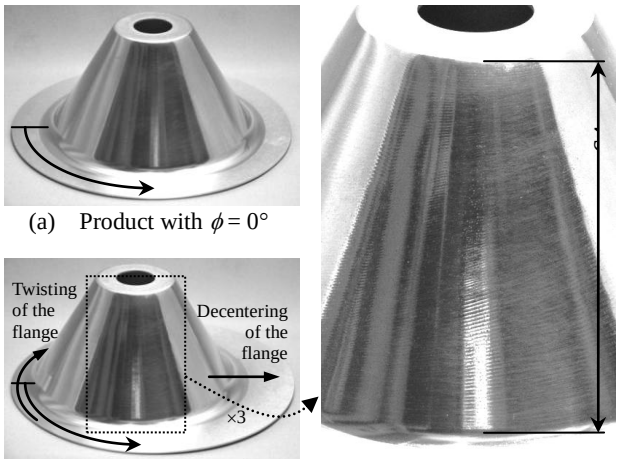

(a) Product with $\phi = 0°$

(b) Product with $\phi = 15°$ (c) Feed marks on the wall

Fig. 11. Comparison of truncated cones with different inclination angles ϕ of the flange in shear spinning.

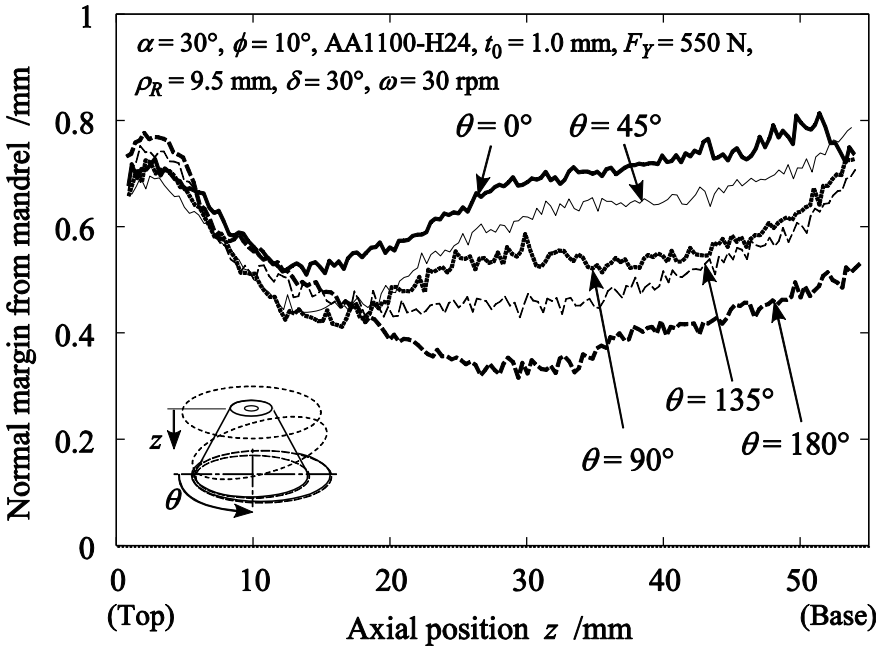

Fig. 12. Normal margin between the profile of the product with ϕ = 10° and the mandrel over half the circumference.

circumferentially rotated 12°–15° from the original blank in the opposite direction to that of the roller feed.

Fig. 12 shows axial distributions of the normal margin between the profile of the product with ϕ =

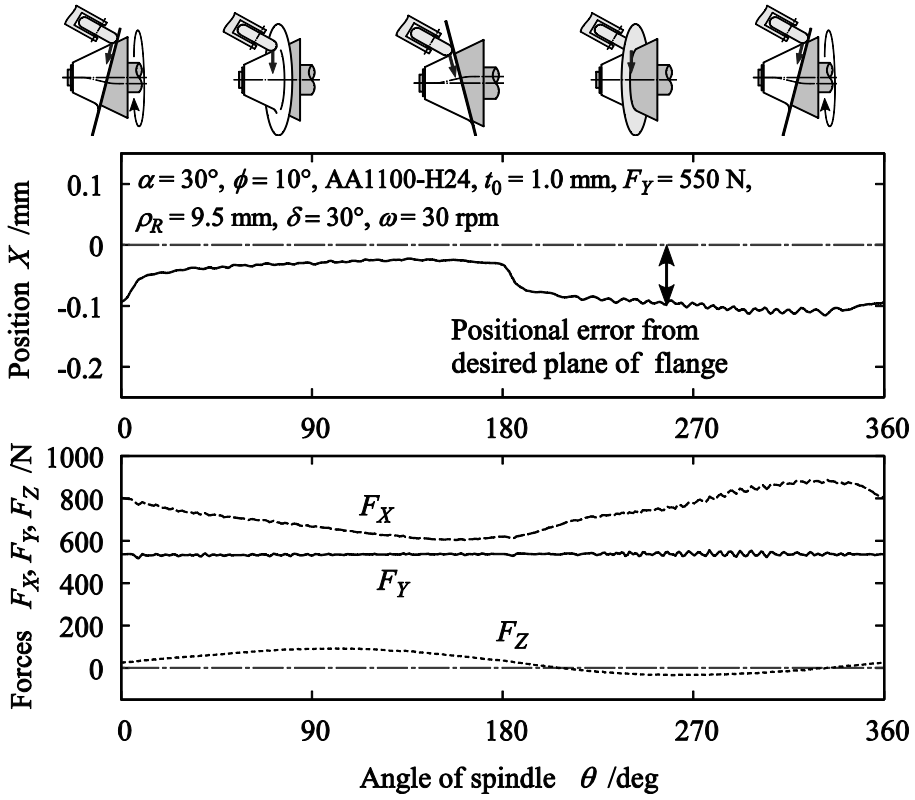

Fig. 13. Positional error of the roller from the desired flange plane and the forces along the circumference of the spindle.

10° and the mandrel over half the circumference. In comparison with axial thickness distributions shown later in **Fig. 14**, the entire surface of the wall remained close to the mandrel. Thus, the outer profiles for different circumferential angles θ are different, since the inner profiles close to the mandrel are conical. However, the accuracy of the profiles obtained by the present process using force control is better than that obtained by the dieless process without springback compensation.

Fig. 13 shows the positional error of the roller from the desired plane of the flange and the forces along the circumference at the intersection between the flange plane inclined at 10° and the spindle axis, 30 mm from the top of the mandrel. Even though the tip shape of the roller is approximated by a sphere to simplify the calculation, there is no problem in conducting the forming while maintaining a flat flange, since the positional error is low (less than about 100 μm). The centripetal force F_Y parallel to the flange plane was maintained close to the desired value of 550 N, and the force normal

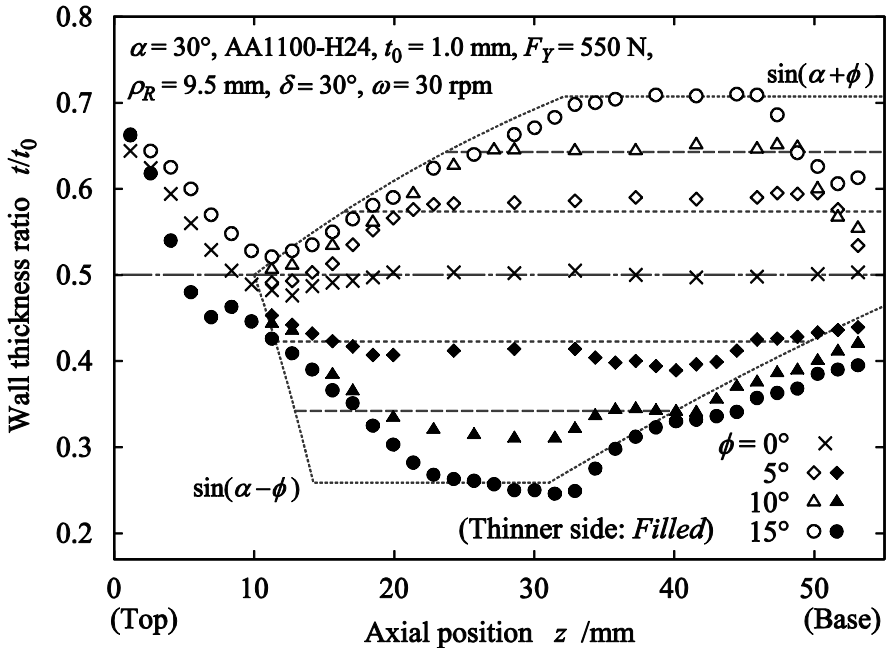

Fig. 14. Axial distributions of wall thickness ratio on thicker and thinner sides for inclination angles ϕ of up to 15°.

to the plane was 800 N on average.

4.4. Axial Distributions of Wall Thickness

Fig. 14 shows axial distributions of the ratio of wall thickness t to original thickness t_0 for inclination angles of ϕ = 0°, 5°, 10°, and 15° along the thicker and thinner sides. The dotted lines in the figure are predictive distributions calculated from the trajectory of the flange plane (the thick dash-dotted line in **Fig. 9**) using Equation (2). Similarly to in the previous dieless process, the ratio at ϕ = 0° is t/t_0 = sin30° = 0.5, while the amount of thinning increases or decreases compared with the ratio of the sine law on each side at greater inclination angles. There are slightly depressed areas on the walls near the points A and B shown in **Fig. 9** at z = 8 and 53 mm.

However, in comparison with **Fig. 6**, the actual axial distribution is backshifted and more complicated, particularly on the thinner side. As the mechanisms understanding these results, the displacement of the material by the nipping of the roller and mandrel and the subsequent thinning of

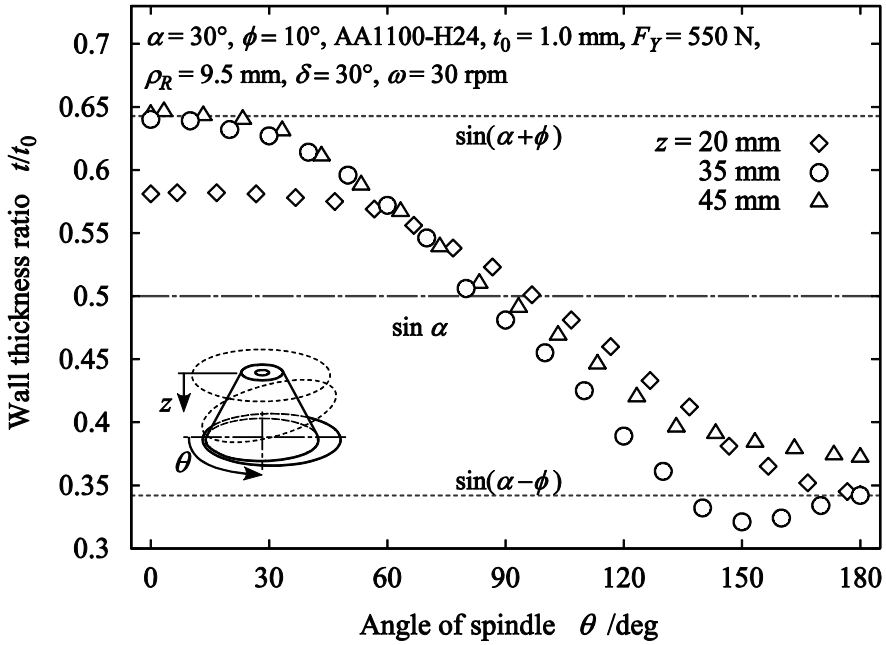

Fig. 15. Circumferential distributions of wall thickness ratio along half circumferences of the cone at various axial positions when $\phi = 10°$.

the preformed wall by the tangential tensile force are considered.

4.5. Circumferential Distributions of Wall Thickness

Fig. 15 shows circumferential distributions of the thickness ratio t/t_0 along half circumferences of the product with $\phi = 10°$ at distances of z = 20, 35, and 45 mm from top of the product. The distributions are essentially the same as those in **Fig. 7** a sinusoidal function whose maximum and minimum values are approximately $\sin(\alpha \pm \phi)$. Moreover the variation from the thickness ratio given by $\sin\alpha$ depends on the inclination angle at the point. However, compared with **Fig. 7**, thickening and thinning are promoted at circumferential angles of $\theta = 30°$ and 150°, respectively. This is attributed to the roller deforming the material onto the wall of the mandrel, which has an elliptical cross section, while twisting the flange in the circumferential direction.

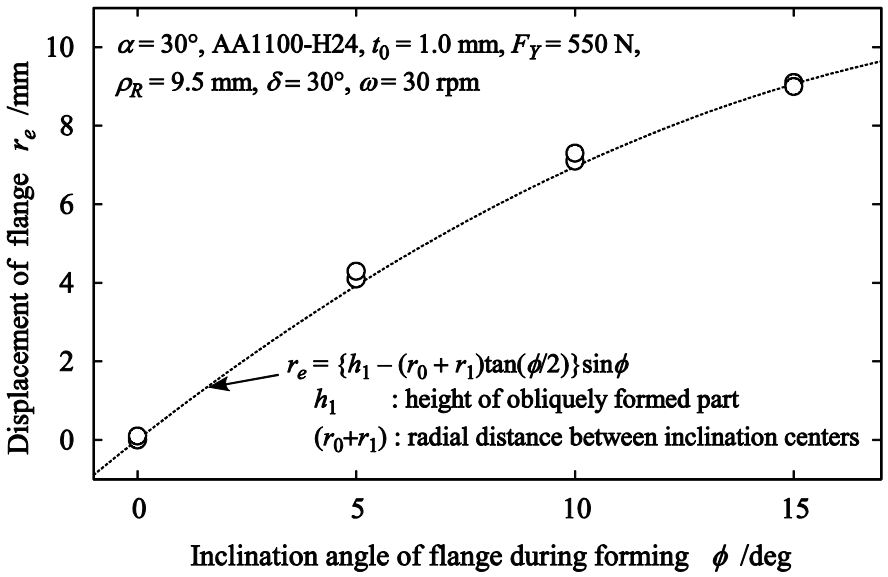

Fig. 16. Relationship between inclination angle ϕ and radial displacement of flange r_e.

4.6. Radial Displacement of Flange

Fig. 16 shows the relationship between the inclination angle ϕ and the displacement of the flange, r_e, which is calculated from the greatest difference between the radial distances from the spindle axis to the hem. The dotted line, which is calculated using Equation (4), was in close agreement with the measured results. Hence, it would appear that the gross variation is the same under the same forming conditions in the dieless and force-controlled processes and is independent of the twist of the flange.

5. Conclusions

In this study, the findings of experiments in which truncated cone products are formed from metal sheet by synchronous dieless spinning and force-controlled shear spinning are summarized as follows:

1. It was revealed that the wall thickness distribution can be varied by changing the inclination angle of the flange from the original plane in the oblique shear spinning processes. The estimated thickness distributions normal to the flange plane based on a simple shear deformation

model nearly coincided with the measured thicknesses along the outer and inner sides of the inclination of flange. The inclination angle affects the ratio of the wall thickness to the original thickness. The circumferential distributions can be passively determined by designing the axial distribution on the major sides.

2. The radial displacements of the flange can be simply calculated in advance, thus reducing material wastage, by offsetting the radial position and the circumferential angle of the blank.

3. The synchronous dieless spinning method is suitable for varying the wall thickness, while the force-controlled shear spinning method has the advantage of higher profile accuracy, which was clarified by comparing the deviations from the desired profiles in **Fig. 5** and **Fig. 12**, and the differences between the actual thicknesses and the estimated values in **Fig. 6** and **Fig. 14**.

Additionally, the results in this study suggest that varying the wall thickness by inclining the flange plane of the workpiece during the process is also practicable in incremental sheet forming processes in which the deformation behavior obeys the sine law, not only in shear spinning.

References

Music, O., Allwood, J.M., Kawai, K., 2010. A review of the mechanics of metal spinning. J. Mater. Process. Technol. 210 (1), 3–23.

Shima, S., Kotera, H., Murakami, H., 1997. Development of flexible spin-forming method. J. Jpn. Soc. Technol. Plastic. (Plastic. Process.) 38 (440), 814–818.

Kawai, K., Yang, L.N., Kudo H., 2001. A flexible shear spinning of truncated conical shells with a general-purpose mandrel. J. Mater. Process. Technol. 113 (1–3), 28–33.

Amano, T., Tamura, K., 1984. The study of an elliptical cone spinning by the trial equipment. In: Kobayashi, M. (Ed.), Proceedings of the 3rd International Conference on Rotary Metalworking Processes, Kyoto, Japan, pp. 213–224.

Gao, X.C., Kang, D.C., Meng, X.F, Wu, H.J., 1999. Experimental research on a new technology—ellipse spinning. J. Mater. Process. Technol. 94 (2–3), 197–200.

Qinxiang, X., Zhouyi, L., Xinxi, Z., Xiuquan, C., 2010. Research on spinning method of hollow part with triangle arc-type cross section based on profiling driving. Steel Research International, Special edition Metal Forming 2010, 81 (9), 994–997.

Arai, H., Fujimura, S., Okazaki, I., 2005. Synchronous metal spinning of non-axisymmetric tubes. In: Proceedings of the 56th Japanese Joint Conference for the Technology of Plasticity, pp. 687–688 (in Japanese).

Amano, T., Mori, S., Tamura, K., 1990. Prototype of computerized elliptical spinning machine, report 1 system configuration and roller trajectory. In: Proceedings of the 1990 Japanese Spring Conference for the Technology of Plasticity, pp. 555–556 (in Japanese).

Härtel, S., Awiszus, B., 2010. Numerical and experimental investigations of production of non-rotationally symmetric hollow parts using sheet metal spinning. Steel Research International, Special edition Metal Forming 2010, 81 (9), 998–1001.

Shimizu, I., 2010. Asymmetric forming of aluminum sheets by synchronous spinning. J. Mater. Process. Technol. 210 (4), 585–592.

Awiszus, B., Meyer, F., 2005. Metal spinning of non-circular hollow parts. In: Bariani, P.F. (Ed.), Proceedings of the 8th International Conference on Technology of Plasticity, Verona, Italy, pp. 353–354.

Arai, H., 2004. Robotic metal spinning—shear spinning using force feedback control. J. Robotics Soc. Jpn. 22 (6), 798–805.

Arai, H., 2005. Robotic metal spinning—forming non-axisymmetric products using force control. In: Proceedings of the 2005 IEEE International Conference on Robotics and Automation, Barcelona, Spain, pp. 2702–2707.

Shindo, K., Ishigaki, K., Kato, K., Irie, T., 1999. Development of novel tube spinning technology (spinning technology for decentered or inclined shapes report 1). In: Proceedings of the 50th Japanese Joint Conference for the Technology of Plasticity, pp. 173–174 (in Japanese).

Xia, Q.X., Cheng, X.Q., Hu, Y., Ruan, F., 2006. Finite element simulation and experimental investigation on the forming forces of 3D non-axisymmetrical tubes spinning. Int. J. Mech. Sci. 48 (7), 726–735.

Matsubara, S., 1994. Incremental backward bulge forming of a sheet metal with a hemispherical head tool—a study of a numerically controlled forming system II. J. Jpn. Soc. Technol. Plastic. (Plastic. Process.) 35 (406), 1311–1321.

Matsubara, S., 1995. Incremental forming of a sheet metal (number 5)—study of forming system using numerically-controlled machine tool report 15. In: Proceedings of the 46th Japanese Joint Conference for the Technology of Plasticity, pp. 33–34 (in Japanese).

Wong, C.C., Dean, T.A., Lin, J., 2003. A review of spinning, shear forming and flow forming processes. Int. J. Mach. Tools Manuf. 43 (14), 1419–1435.

Sekiguchi, A., Arai, H., 2010a. Synchronous die-less spinning of curved products. Steel Research International, Special edition Metal Forming 2010, 81 (9), 1010–1013.

Sekiguchi, A., Arai, H., 2010b. Development of oblique metal spinning with force control. In: Proceedings of 2010 International Symposium on Flexible Automation, Tokyo, Japan, JPL-2453.

Graphical abstract

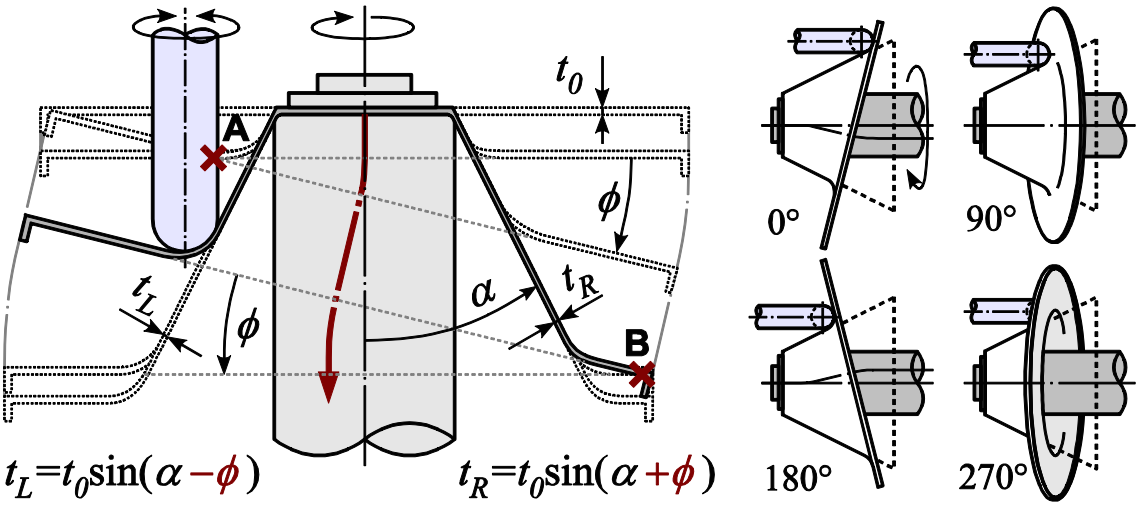

Highlights

- A flexible method of forming variant wall thickness distributions is proposed.
- Thickness varies by changing inclination angle of flange in oblique shear spinning.
- Major thickness can be calculated in advance based on a shear deformation model.
- Radial displacement of flange can be simply estimated from forming conditions.

Figure captions

Fig. 1. Relationship among the half-angle α, the inclination angle ϕ, and the wall thicknesses in the oblique shear deformation model.

Fig. 2. Schematic of the experiment on controlling the wall thickness distribution in synchronous dieless spinning.

Fig. 3. Synchronous motion of the tool during one rotation of the spindle.

Fig. 4. Comparison of truncated cones with different inclination angles ϕ of the flange in dieless forming.

Fig. 5. Normal deviation of the outer profile of the product with ϕ = 15° from the desired profile over half the circumference.

Fig. 6. Axial distributions of wall thickness ratio on thicker and thinner sides for inclination angles ϕ of up to 15°.

Fig. 7. Circumferential distributions of wall thickness ratio along half circumferences of the cone at various axial positions when ϕ = 10°.

Fig. 8. Relationship between inclination angle ϕ and radial displacement of flange *re*.

Fig. 9. Schematic of the experiment on controlling the wall thickness distribution in force-controlled shear spinning.

Fig. 10. Motion of the roller and the constant-force direction during one rotation in force-controlled shear spinning.

Fig. 11. Comparison of truncated cones with different inclination angles ϕ of the flange in shear spinning.

Fig. 12. Normal margin between the profile of the product with ϕ = 10° and the mandrel over half the circumference.

Fig. 13. Positional error of the roller from the desired flange plane and the forces along the circumference of the spindle.

Fig. 14. Axial distributions of wall thickness ratio on thicker and thinner sides for inclination angles ϕ of up to 15°.

Fig. 15. Circumferential distributions of wall thickness ratio along half circumferences of the cone at various axial positions when ϕ = 10°.

Fig. 16. Relationship between inclination angle ϕ and radial displacement of flange *re*.

Table captions

Table 1

Mechanical properties of aluminum disc of 1.5 mm thickness using specimen #6 of JIS. 2201.

Table 2

Mechanical properties of aluminum disc of 1.0 mm thickness using specimen #6 of JIS. 2201.